Matter-wave squeezing and the generation of SU(1,1) and SU(2) coherent states via Feshbach resonances

I. Tikhonenkov, E. Pazy, Y. B. Band, and A. Vardi

Department of Chemistry, Ben Gurion University of Negev, P.O. Box 653, Beer Sheva 84105, Israel

(Received 22 October 2007; published 24 June 2008)

Pair operators for boson and fermion atoms generate SU(1,1) and SU(2) Lie algebras, respectively. Consequently, the pairing of boson and fermion atoms into diatomic molecules via Feshbach resonances, produces SU(1,1) and SU(2) coherent states, making bosonic pairing the matter-wave equivalent of parametric coupling and fermion pairing equivalent to the Dicke model of quantum optics. We discuss the properties of atomic states generated in the dissociation of molecular Bose-Einstein condensates into boson or fermion constituent atoms. The SU(2) coherent states produced in dissociation into fermions give Poissonian atom-number distributions, whereas the SU(1,1) states generated in dissociation into bosons result in super-Poissonian distributions, in analogy to two-photon squeezed states. In contrast, starting from an atomic gas produces coherent number distributions for bosons and super-Poissonian distributions for fermions.

I. INTRODUCTION

The behavior of a gas of noninteracting particles close to the absolute zero of temperature depends solely on their quantum statistics. Whereas fermions obey Pauli exclusion, manifested in the equal-time anticommutation relations of their field operators, bosons are subject to Bose enhancement, implicit in their field operator commutators. For interacting particles, the interaction affects the pair-statistics of fermions and bosons. Pairing models have attracted renewed interest since Feshbach resonances [1,2] have been employed to realize molecular Bose-Einstein condensates with fermionic [3–6] and bosonic [7–9] constituent atoms, and the ensuing research of the BEC-BCS crossover [10–17]. Recently, some attention was given to the relation between the quantum statistics of the atomic gas in which Feshbach or optical association is performed, and the resulting number-statistics of the atomic and molecular fields generated in the process [18–24]. It was shown that, whereas the molecular field produced in boson association will initially be in a Glauber coherent state $|\alpha\rangle$, defined such that $a|\alpha\rangle = \alpha|\alpha\rangle$ where a is a destruction operator, having Poissonian particle-number fluctuations [i.e., $(\Delta n)^2/\langle n\rangle = 1$, where $n = a^\dagger a$ and $(\Delta n)^2 = \langle n^2\rangle - \langle n\rangle^2$], the corresponding number distributions for fermions will be super-Poissonian [22] with $(\Delta n)^2$ exceeding $\langle n\rangle$. The coherence of the boson-association field was attributed to collective association, whereas the chaotic number distributions for fermion association were related to the individual association of fermionic atom pairs.

Here we explain and quantify these differences in the molecular number-statistics in terms of the commutation relations of fermion and boson pair operators. It is well known that pair operators for fermions and bosons generate SU(2) and SU(1,1) algebras, respectively [25–27]. Consequently, the atomic field produced in the dissociation of a molecular BEC into fermion atoms will be in an SU(2) coherent state with Poissonian number distribution, whereas boson atoms thus generated, will be in a SU(1,1) coherent state, corresponding to a squeezed state of the Heisenberg-Weyl algebra, with a super-Poissonian distribution. Using the simple map-

ping between SU(2) and SU(1,1) it is shown that for association, SU(1,1) coherent states will initially dominate fermion pairing whereas SU(2) states will be generated for bosons. Boson association (unlike boson dissociation) is not a collective effect since the atomic field can be initially replaced by a constant macroscopic c number, rendering the initial molecule production process perfectly linear. The super-Poissonian statistics of fermion association, on the other hand, actually result from collective behavior of the fermionic association. In particular, it will also show up in the degenerate fermionic case, where all atom pairs "emit" molecules in-phase.

In Sec. II we discuss the dynamical equations for associative pairing of fermionic and bosonic atoms. Section III describes the bosonic and fermionic coherent states of the SU(1,1) and SU(2) algebras generated by the angular-momentum-like operators, respectively. Section IV discusses the short time dynamics of the dissociation of a molecular BEC into bosonic and fermionic atoms. Section V concludes the paper.

II. DYNAMICAL EQUATIONS

We begin by considering the dynamical equations for associative pairing of fermionic and bosonic atoms, highlighting similarities and differences resulting from the underlying pair statistics of SU(2) for fermions and of SU(1,1) for bosons. As shown below, when the atomic motion is slow with respect to other timescales, the atom-molecule pairing Hamiltonians map onto two quantum-optical paradigmatic systems; The pairing of fermion atoms [19–24,26–30] is a matter-wave equivalent of Dicke superradiance [31], whereas the dissociation into bosonic atoms [18,24,32–43] is analogous to parametric down-conversion [44].

A. Fermion atoms—SU(2) algebra

Consider the single molecular mode association/dissociation Hamiltonian

$$H = \sum_{\mathbf{k},\sigma} \epsilon_{\mathbf{k}} c_{\mathbf{k},\sigma}^{\dagger} c_{\mathbf{k},\sigma} + \mathcal{E} b^{\dagger} b + \left(g b^{\dagger} \sum_{\mathbf{k}} c_{\mathbf{k},\uparrow} c_{-\mathbf{k},\downarrow} + \text{H.c.} \right), \quad (1)$$

where $\epsilon_{\mathbf{k}} = \hbar^2 k^2 / 2m$ is the kinetic energy of an atom with mass m, $\mathcal{E}$ is the molecular energy, containing kinetic and binding contributions, and g is the atom-molecule coupling strength, which will be assumed real for simplicity throughout this section. The extension to an arbitrary phase φ of g is straightforward. The annihilation operators for the atoms $c_{\mathbf{k},\sigma}$ obey fermionic anticommutation relations, whereas the molecular annihilation operator b obeys a bosonic commutation relation. The single mode approximation is justified when the molecular dispersion due to the presence of a molecular momentum spread, is slow with respect to any other timescale in the problem. It becomes exact for a molecular BEC, when molecular translation is completely frozen. For simplicity, we have also omitted background nonreactive atom-atom scattering. As will be evident from the discussion below, these interactions can be easily incorporated, as long as they are dominated by $(\mathbf{k}\uparrow, -\mathbf{k}\downarrow)$ pairing. While this assumption is well justified for fermions in the BCS state, it is a gross oversimplification for bosons. We thus expect that our results will be restricted to the case where background open-channel interactions are small with respect to closed-channel atom-molecule coupling, i.e., to narrow Feshbach resonances.

For fermionic atomic field operators, the model Hamiltonian (1) can be written using only the atomic SU(2) generators [26,27]

$$S_{-}^{\mathbf{k}} = c_{\mathbf{k},\uparrow} c_{-\mathbf{k},\downarrow}, \quad S_{+}^{\mathbf{k}} = c_{-\mathbf{k},\downarrow}^{\dagger} c_{\mathbf{k},\uparrow}^{\dagger},$$

$$S_{z}^{\mathbf{k}} = \frac{1}{2} (-1 + c_{\mathbf{k},\uparrow}^{\dagger} c_{\mathbf{k},\uparrow} + c_{-\mathbf{k},\downarrow}^{\dagger} c_{-\mathbf{k},\downarrow}), \quad (2)$$

obeying the canonical angular-momentum commutation relations

$$[S_{+}^{\mathbf{k}}, S_{-}^{\mathbf{k}}] = 2S_{z}^{\mathbf{k}}, \quad [S_{z}^{\mathbf{k}}, S_{\pm}^{\mathbf{k}}] = \pm S_{\pm}^{\mathbf{k}}. \quad (3)$$

Using Eqs. (2), Hamiltonian (1) may be rewritten as

$$H = \sum_{\mathbf{k}} \epsilon_{\mathbf{k}} (2S_{z}^{\mathbf{k}} + 1) + \mathcal{E} b^{\dagger} b + g \sum_{\mathbf{k}} (b^{\dagger} S_{-}^{\mathbf{k}} + S_{+}^{\mathbf{k}} b), \quad (4)$$

resulting in the Heisenberg equations of motion

$$i\dot{S}_{+}^{\mathbf{k}} = [S_{+}^{\mathbf{k}}, H] = -2\epsilon_{\mathbf{k}} S_{+}^{\mathbf{k}} + 2g b^{\dagger} S_{z}^{\mathbf{k}},$$

$$i\dot{S}_{-}^{\mathbf{k}} = [S_{-}^{\mathbf{k}}, H] = 2\epsilon_{\mathbf{k}} S_{-}^{\mathbf{k}} - 2g S_{z}^{\mathbf{k}} b,$$

$$i\dot{S}_{z}^{\mathbf{k}} = [S_{z}^{\mathbf{k}}, H] = g(S_{+}^{\mathbf{k}} b - b^{\dagger} S_{-}^{\mathbf{k}}),$$

$$i\dot{b} = [b, H] = \mathcal{E} b + g \sum_{\mathbf{k}} S_{-}^{\mathbf{k}}. \quad (5)$$

Defining the Hermitian operators

$$S_{x}^{\mathbf{k}} = \frac{S_{+}^{\mathbf{k}} + S_{-}^{\mathbf{k}}}{2}, \quad S_{y}^{\mathbf{k}} = \frac{S_{+}^{\mathbf{k}} - S_{-}^{\mathbf{k}}}{2i}, \quad B_{x} = \frac{b + b^{\dagger}}{2}, \quad B_{y} = \frac{b - b^{\dagger}}{2i}.$$

$$(6)$$

Equation (5) transforms into

$$\dot{S}_{x}^{\mathbf{k}} = -2\epsilon_{\mathbf{k}} S_{y}^{\mathbf{k}} - 2g B_{y} S_{z}^{\mathbf{k}}, \quad \dot{S}_{y}^{\mathbf{k}} = 2\epsilon_{\mathbf{k}} S_{x}^{\mathbf{k}} - 2g B_{x} S_{z}^{\mathbf{k}},$$

$$\dot{S}_{z}^{\mathbf{k}} = 2g(B_{x} S_{y}^{\mathbf{k}} + B_{y} S_{x}^{\mathbf{k}}), \quad \dot{B}_{x} = \mathcal{E} B_{y} - g \sum_{\mathbf{k}} S_{y}^{\mathbf{k}},$$

$$\dot{B}_{y} = -\mathcal{E} B_{x} - g \sum_{\mathbf{k}} S_{x}^{\mathbf{k}}. \quad (7)$$

System (7) satisfies the conservation of the individual spin angular momenta, with the SU(2) Casimir operators

$$\mathbf{S}^{\mathbf{k}2} = S_{z}^{\mathbf{k}} (S_{z}^{\mathbf{k}} - 1) + S_{+}^{\mathbf{k}} S_{-}^{\mathbf{k}} = s(s+1), \quad (8)$$

with $s = 1/2$, as well as total number conservation

$$(B_{x}^{2} + B_{y}^{2} - 1/2) + \sum_{\mathbf{k}} (S_{z}^{\mathbf{k}} + 1/2) = N/2, \quad (9)$$

where $N = 2b^{\dagger} b + \sum_{\mathbf{k},\sigma} c_{\mathbf{k},\sigma}^{\dagger} c_{\mathbf{k},\sigma}$. Defining,

$$\mathcal{S}_{+}^{\mathbf{k}} = S_{+}^{\mathbf{k}} b, \quad \mathcal{S}_{-}^{\mathbf{k}} = b^{\dagger} S_{-}^{\mathbf{k}}, \quad (10)$$

the dynamical Eq. (5) take the form

$$i\dot{\mathcal{S}}_{+}^{\mathbf{k}} = \Delta_{\mathbf{k}} \mathcal{S}_{+}^{\mathbf{k}} + 2g b^{\dagger} b S_{z}^{\mathbf{k}} + g \sum_{\mathbf{k}'} S_{+}^{\mathbf{k}} S_{-}^{\mathbf{k}'},$$

$$i\dot{\mathcal{S}}_{-}^{\mathbf{k}} = -\Delta_{\mathbf{k}} \mathcal{S}_{-}^{\mathbf{k}} - 2g b^{\dagger} b S_{z}^{\mathbf{k}} - g \sum_{\mathbf{k}'} S_{+}^{\mathbf{k}'} S_{-}^{\mathbf{k}},$$

$$i\dot{S}_{z}^{\mathbf{k}} = g(\mathcal{S}_{+}^{\mathbf{k}} - \mathcal{S}_{-}^{\mathbf{k}}), \quad (11)$$

with $\Delta_{\mathbf{k}} = \mathcal{E} - 2\epsilon_{\mathbf{k}}$.

For the degenerate case $\epsilon_{\mathbf{k}} \to \epsilon$, which yields

$$\Delta_{\mathbf{k}} \to \Delta = \mathcal{E} - 2\epsilon. \quad (12)$$

Hamiltonian (4) is, up to an insignificant c-number shift, just the Dicke Hamiltonian [31] and the dynamical equations become

$$i\dot{\mathcal{J}}_{+} = \Delta \mathcal{J}_{+} + 2g b^{\dagger} b J_{z} + g J_{+} J_{-},$$

$$i\dot{\mathcal{J}}_{-} = -\Delta \mathcal{J}_{-} - 2g b^{\dagger} b J_{z} - g J_{+} J_{-},$$

$$i\dot{J}_{z} = g(\mathcal{J}_{+} - \mathcal{J}_{-}), \quad (13)$$

where $J_{i} = \sum_{\mathbf{k}} S_{i}^{\mathbf{k}}$, $\mathcal{J}_{i} = \sum_{\mathbf{k}} \mathcal{S}_{i}^{\mathbf{k}}$. In order to get a closed set of equations for $\mathcal{J}_{+}$, $\mathcal{J}_{-}$, and J_{z}, we use the SU(2) Casimir operator

$$J_{z}(J_{z} - 1) + J_{+} J_{-} = j(j+1) \quad (14)$$

and number conservation

$$b^{\dagger} b = \frac{N}{2} - (j + J_{z}), \quad (15)$$

where $N = 2b^{\dagger} b + \sum_{\mathbf{k},\sigma} c_{\mathbf{k},\sigma}^{\dagger} c_{\mathbf{k},\sigma}$ is the total number of atoms and j is the number of available energy levels (containing at most $4j$ particles, because each level can accommodate $\mathbf{k}\uparrow, \mathbf{k}\downarrow, -\mathbf{k}\uparrow, -\mathbf{k}\downarrow$ atoms). Substituting Eqs. (14) and (15) into Eq. (13), we obtain

$$i\dot{\mathcal{J}}_+ = \Delta\mathcal{J}_+ - g[3J_z^2 - (N - 2j)J_z - j^2 - j - J_z],$$

$$i\dot{\mathcal{J}}_- = -\Delta\mathcal{J}_- + g[3J_z^2 - (N - 2j)J_z - j^2 - j - J_z],$$

$$i\dot{J}_z = g(\mathcal{J}_+ - \mathcal{J}_-). \tag{16}$$

Defining the normalized operators

$$\mathcal{J}_x = \frac{\mathcal{J}_+ + \mathcal{J}_-}{2(N/4)^{3/2}}, \quad \mathcal{J}_y = \frac{\mathcal{J}_+ - \mathcal{J}_-}{2i(N/4)^{3/2}}, \quad \mathcal{J}_z = \frac{J_z}{N/4}, \tag{17}$$

we finally obtain the dynamical equations

$$\dot{\mathcal{J}}_x = \Delta\mathcal{J}_y, \tag{18}$$

$$\dot{\mathcal{J}}_y = -\Delta\mathcal{J}_x + \frac{g\sqrt{N}}{2}[3\mathcal{J}_z^2 - (4 - 2\eta)\mathcal{J}_z - \eta^2] - \frac{2g}{\sqrt{N}}(\eta + \mathcal{J}_z), \tag{19}$$

$$\dot{\mathcal{J}}_z = g\sqrt{N}\mathcal{J}_y, \tag{20}$$

where $\eta = 4j/N$ denotes the number of quantum states per particle or the inverse phase space density. For a thermal gas $\eta \gg 1$, whereas for a Fermi degenerate gas $\eta = 1$. For a filled Fermi sea, η attains its minimal value of unity, and Eq. (19) can be replaced by

$$\dot{\mathcal{J}}_y = -\Delta\mathcal{J}_x - \frac{g\sqrt{N}}{2}[(1 - \mathcal{J}_z)(1 + 3\mathcal{J}_z)] - \frac{2g}{\sqrt{N}}(1 + \mathcal{J}_z). \tag{21}$$

B. Boson atoms—SU(1,1) algebra

We next consider the coupling of a molecular BEC into bosonic atom pairs. The single molecular mode Hamiltonian reads

$$H = \sum_{\mathbf{k},\sigma} \epsilon_{\mathbf{k}} a_{\sigma,\mathbf{k}}^\dagger a_{\sigma,\mathbf{k}} + \mathcal{E}b^\dagger b + g\left(b^\dagger \sum_{\mathbf{k}} a_{1,\mathbf{k}} a_{2,-\mathbf{k}} + \text{H.c.}\right), \tag{22}$$

where $\epsilon_{\mathbf{k}}$, $\mathcal{E}$, g, and b have the same meaning as in Eq. (1) and the atomic annihilation operators $a_{\sigma,\mathbf{k}}$, denoting two atom species, now obey bosonic commutation relations.

The pertinent algebra for bosonic atom operators is SU(1,1), because the commutator of $K_-^{\mathbf{k}} = a_{1,\mathbf{k}} a_{2,-\mathbf{k}}$ and $K_+^{\mathbf{k}} = a_{2,-\mathbf{k}}^\dagger a_{1,\mathbf{k}}^\dagger$ is

$$[K_+^{\mathbf{k}}, K_-^{\mathbf{k}}] = (-1 - a_{1,\mathbf{k}}^\dagger a_{1,\mathbf{k}} - a_{2,-\mathbf{k}}^\dagger a_{2,-\mathbf{k}}) \equiv -2K_z^{\mathbf{k}}, \tag{23}$$

so that the three generators $K_+^{\mathbf{k}}, K_-^{\mathbf{k}}, K_z^{\mathbf{k}}$ obey SU(1,1) commutation relations

$$[K_+^{\mathbf{k}}, K_-^{\mathbf{k}}] = -2K_z^{\mathbf{k}}, \quad [K_z^{\mathbf{k}}, K_\pm^{\mathbf{k}}] = \pm K_\pm^{\mathbf{k}}, \tag{24}$$

differing only in the sign of $[K_+^{\mathbf{k}}, K_-^{\mathbf{k}}]$ from the commutation relation between the SU(2) generators, stipulated in Eq. (3). Hamiltonian (4) is thus replaced by the SU(1,1) Hamiltonian

$$H = \sum_{\mathbf{k}} \epsilon_{\mathbf{k}}(2K_z^{\mathbf{k}} - 1) + \mathcal{E}b^\dagger b + g\sum_{\mathbf{k}}(b^\dagger K_-^{\mathbf{k}} + K_+^{\mathbf{k}}b), \tag{25}$$

leading to the Heisenberg equations of motion

$$i\dot{K}_+^{\mathbf{k}} = [K_+^{\mathbf{k}}, H] = -2\epsilon_{\mathbf{k}}K_+^{\mathbf{k}} - 2gb^\dagger K_z^{\mathbf{k}},$$

$$i\dot{K}_-^{\mathbf{k}} = [K_-^{\mathbf{k}}, H] = 2\epsilon_{\mathbf{k}}K_-^{\mathbf{k}} + 2gK_z^{\mathbf{k}}b,$$

$$i\dot{K}_z^{\mathbf{k}} = [K_z^{\mathbf{k}}, H] = g(K_+^{\mathbf{k}}b - b^\dagger K_-^{\mathbf{k}}),$$

$$i\dot{b} = [b, H] = \mathcal{E}b + g\sum_{\mathbf{k}} K_-^{\mathbf{k}}. \tag{26}$$

For degenerate atomic energy levels, the boson Hamiltonian (25) is identical to the model Hamiltonian of parametric down-conversion [44]. Following the same procedure as in the previous section, we obtain for boson degenerate modes

$$i\dot{\mathcal{K}}_+ = \Delta\mathcal{K}_+ - 2gb^\dagger bK_z + gK_+K_-,$$

$$i\dot{\mathcal{K}}_- = -\Delta\mathcal{K}_- + 2gb^\dagger bK_z - gK_+K_-,$$

$$i\dot{K}_z = g(\mathcal{K}_+ - \mathcal{K}_-), \tag{27}$$

where $K_\pm = \Sigma_{\mathbf{k}}K_\pm^{\mathbf{k}}$, $K_z = \Sigma_{\mathbf{k}}K_z^{\mathbf{k}}$, $\mathcal{K}_+ = K_+b$, and $\mathcal{K}_- = b^\dagger K_-$. In contrast to the unitary SU(2) case where we had

$$-j \leq \langle J_z \rangle \leq -j + \min\{N/2, 2j\},$$

reducing to $-j \leq \langle J_z \rangle \leq j$ for $N = 4j$, we now have

$$k \leq \langle K_z \rangle \leq k + N/2,$$

where $4k$ denotes the number of boson atomic modes. However, we can still eliminate $K_\pm$ and b by using number conservation and the SU(1,1) Casimir operator

$$b^\dagger b = \frac{N}{2} - (K_z - k), \tag{28}$$

$$K_z(K_z - 1) - K_+K_- = k(k - 1), \tag{29}$$

resulting in the dynamical equations

$$i\dot{\mathcal{K}}_+ = \Delta\mathcal{K}_+ + g[3K_z^2 - (N + 2k)K_z - k^2 + k - K_z],$$

$$i\dot{\mathcal{K}}_- = -\Delta\mathcal{K}_- - g[3K_z^2 - (N + 2k)K_z - k^2 + k - K_z],$$

$$i\dot{K}_z = g(\mathcal{K}_+ - \mathcal{K}_-). \tag{30}$$

We define, as we did for fermion atoms,

$$\mathcal{K}_x = \frac{\mathcal{K}_+ + \mathcal{K}_-}{2(N/4)^{3/2}}, \quad \mathcal{K}_y = \frac{\mathcal{K}_+ - \mathcal{K}_-}{2i(N/4)^{3/2}}, \quad \mathcal{K}_z = \frac{K_z}{(N/4)}, \tag{31}$$

and using these definitions, the dynamical equations are transformed to the final form

$$\dot{\mathcal{K}}_x = \Delta\mathcal{K}_y,$$

$$\dot{\mathcal{K}}_y = -\Delta\mathcal{K}_x - \frac{g\sqrt{N}}{2}[3\mathcal{K}_z^2 - (4+2\eta)\mathcal{K}_z - \eta^2] + \frac{2g}{\sqrt{N}}(\mathcal{K}_z - \eta),$$

$$\dot{\mathcal{K}}_z = g\sqrt{N}\mathcal{K}_y. \tag{32}$$

In order to gain better insight on the relation between the fermion equation (20) and the boson equation (32) we define the number difference operator $\mathcal{L}_z = (2n_b - n_a)/N = 1 + \eta - \mathcal{K}_z$, whose expectation value, similar to the expectation value of $\mathcal{J}_z$, corresponds to the atom-molecule population imbalance. With this definition, we have

$$3\mathcal{K}_z^2 - (4+2\eta)\mathcal{K}_z - \eta^2 = 3\mathcal{L}_z^2 - (2+4\eta)\mathcal{L}_z - 1, \tag{33}$$

$$\mathcal{K}_z - \eta = 1 - \mathcal{L}_z, \tag{34}$$

and the dynamical Eqs. (32) assume the form

$$\dot{\mathcal{K}}_x = \Delta\mathcal{K}_y,$$

$$\dot{\mathcal{K}}_y = -\Delta\mathcal{K}_x - \frac{g\sqrt{N}}{2}(3\mathcal{L}_z + 1)(\mathcal{L}_z - 1) + \frac{2g}{\sqrt{N}}[(4k-1)\mathcal{L}_z + 1],$$

$$\dot{\mathcal{L}}_z = -g\sqrt{N}\mathcal{K}_y. \tag{35}$$

The two atomic-modes case with Hamiltonian

$$H = \epsilon(a_1^\dagger a_1 + a_2^\dagger a_2) + \mathcal{E}b^\dagger b + g(b^\dagger a_1 a_2 + a_2^\dagger a_1^\dagger b) \tag{36}$$

is obtained from Eq. (35) by substituting $k = 1/2$ (because the minimum value of K_z, obtained where no atoms are present, is $1/2$). It is easily verified that the resulting equations of motion for $\mathcal{K}_x, \mathcal{K}_y, \mathcal{L}_z$ are identical up to the sign of g, with the fermion equations for $\mathcal{J}_x, \mathcal{J}_y, \mathcal{J}_z$ when $\eta = 1$. Noting that $\mathcal{J}_z$ for $\eta = 1$ and $\mathcal{L}_z$ have inverse interpretation [i.e., the former equals $(n_a - 2n_b)/N$ and the latter is $(2n_b - n_a)/N$] we see that the dynamics of degenerate fermion association maps into two-mode boson dissociation and vice versa [45].

III. COHERENT STATES

Having developed the time-dependent many-body formalism and established the connection with the quantum-optical paradigms, we turn to the investigation of the dissociation of a molecular BEC consisting either of fermionic or bosonic constituent atoms. For sufficiently short times, we neglect molecular fluctuations and treat the molecular field b as an undepleted pump, replacing it by the c number $\sqrt{N/2}$. The resulting Hamiltonian for fermion (boson) atoms under this approximation, thus consists of linear sums of operators generating the SU(2) [SU(1,1)] algebra. Consequently, generalized coherent matter states of the pertinent Lie algebras [25], can be dynamically generated in the dissociation of molecular BECs. In this section we briefly discuss the properties of SU(2) [SU(1,1)] coherent states generated in the dissociation of a molecular BEC into fermion (boson) atoms.

A. SU(2) coherent states

The generalized coherent states associated with the unitary representations of the SU(2) Lie algebra, are param-
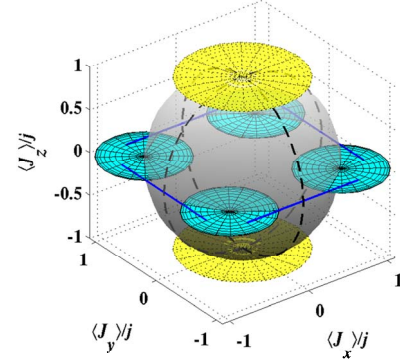

FIG. 1. (Color online) Bloch sphere (shaded shell) and coherent states of SU(2). Dashed black curves mark intelligent coherent states. Ellipses denote ΔJ_x and ΔJ_y variance for ten coherent states: the atomic and molecular vacuum states (large yellow disks), four nonintelligent states (smaller cyan disks) and the four squeezed, minimum uncertainty states (solid blue lines).

etrized by the two polar (Euler) angles θ and ϕ corresponding to rotations of the fully stretched atomic vacuum state $|j,-j\rangle$ (where $|j,m\rangle$ denote the usual mutual eigenstates of the Casimir operator $\mathbf{J}^2$ and of the number difference operator J_z, i.e., $\mathbf{J}^2|j,m\rangle = j(j+1)|j,m\rangle$, $J_z|j,m\rangle = m|j,m\rangle$ with $m = -j, \dots, j$) about the J_y and J_z axes, respectively:

$$|\theta,\phi\rangle \equiv \exp(-i\phi J_z)\exp(-i\theta J_y)|j,-j\rangle$$
$$= \exp(\alpha J_+ - \alpha^* J_-)|j,-j\rangle, \tag{37}$$

with $\alpha = (\theta/2)\exp(-i\phi)$ [46]. Definition (37) results in the familiar expansion of SU(2) coherent states in terms of number (Fock) states

$$|\theta,\phi\rangle = \left[1 + \tan^2\left(\frac{\theta}{2}\right)\right]^{-j} \sum_{m=-j}^{j} \left[\tan\left(\frac{\theta}{2}\right)\exp(-i\phi)\right]^{j+m}$$
$$\times \binom{2j}{j+m}^{1/2} |j,m\rangle. \tag{38}$$

Using either Eq. (37) or Eq. (38) it is easily verified that

$$\langle J_x\rangle = j\sin\theta\cos\phi, \tag{39}$$

$$\langle J_y\rangle = j\sin\theta\sin\phi, \tag{40}$$

$$\langle J_z\rangle = j\cos\theta, \tag{41}$$

so that the expectation values of $\mathbf{J}$ are restricted to the Bloch sphere of radius j, as depicted in Fig. 1. The coherent state variance of these operators is

$$\Delta J_x^2 = \frac{j}{2}(1 - \sin^2\theta\cos^2\phi), \tag{42}$$

$$\Delta J_y^2 = \frac{j}{2}(1 - \sin^2\theta\sin^2\phi), \tag{43}$$

$$\Delta J_z^2 = \frac{j}{2} \sin^2 \theta. \tag{44}$$

The total variance of coherent states is thus also bound because $|\Delta \mathbf{J}|^2 = \langle \mathbf{J}^2 \rangle - \langle \mathbf{J} \rangle^2 = j(j+1) - j^2 = j$. The commutation relations (3), lead to the uncertainty relations

$$\Delta J_i \Delta J_j \geq \frac{1}{2} |c_{ij}^k \langle J_k \rangle|, \tag{45}$$

where $c_{ij}^k = \epsilon_{ij}^k$ are the SU(2) structure constants. In particular, for J_x and J_y we have

$$\Delta J_x \Delta J_y \geq \frac{1}{2} |\langle J_z \rangle|. \tag{46}$$

In Fig. 1 we plot the expectation values of $\mathbf{J}/j = (u, v, w)$ for SU(2) coherent states, as well as the ΔJ_x and ΔJ_y variance of ten such states. Coherent states for which inequality (46) is an equality are referred to as "intelligent states" or "ideal coherent states." From Eqs. (42), (43), and (41) we obtain that SU(2) intelligent states are found for $\phi = 0$, $\pi/2$, π, $3\pi/2$, and arbitrary θ, as depicted by dashed curves in Fig. 1. A subset of the intelligent states are the minimum uncertainty states with $\phi = 0, \pi/2$, π, $3\pi/2$, and $\theta = \pi/2$ (denoted by solid blue lines in Fig. 1), for which the right-hand side of Eq. (46) is minimized, with $\Delta J_x \Delta J_y = 0$. While the states with $\theta = 0$ and ϕ arbitrary (large yellow disks) are also intelligent, their value of $\Delta J_x \Delta J_y = j/2$ is in fact maximal and larger than $\Delta J_x \Delta J_y = j/4$ obtained for the nonintelligent states denoted by smaller cyan disks.

B. SU(1,1) coherent states

The mutual eigenstates of the SU(1,1) Casimir operator (29) and of K_z form the basis set

$$[K_z^2 - K_x^2 - K_y^2]|k,n\rangle = k(k-1)|k,n\rangle, \tag{47}$$

$$K_z |k,n\rangle = (k+n)|k,n\rangle, \tag{48}$$

with $n = 0, 1, \ldots, N/2$. In analogy to Eq. (37), SU(1,1) coherent states are obtained as

$$|\theta, \phi\rangle \equiv \exp(\beta K_+ - \beta^* K_-)|k,0\rangle, \tag{49}$$

with $\beta = -(\theta/2)\exp(-i\phi)$ [47]. Power-series expansion of the exponents in Eq. (49) gives the SU(1,1) coherent states in terms of the number states $|k,n\rangle$,

$$|\theta, \phi\rangle = \left[1 - \tanh^2\left(\frac{\theta}{2}\right)\right]^k \sum_{n=0}^{N/2} \left[-\tanh\left(\frac{\theta}{2}\right)\exp(-i\phi)\right]^n$$

$$\times \left(\frac{\Gamma(n+2k)}{n!\,\Gamma(2k)}\right)^{1/2}|k,n\rangle. \tag{50}$$

Consequently, the expectation values of $\mathbf{K}$ are

$$\langle K_x \rangle = k \sinh \theta \cos \phi, \tag{51}$$

$$\langle K_y \rangle = k \sinh \theta \sin \phi, \tag{52}$$
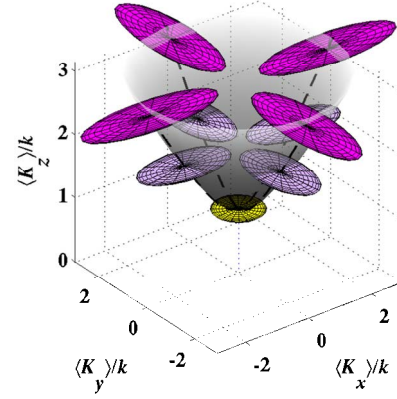

FIG. 2. (Color online) Surface of motion of $\langle \mathbf{K} \rangle / k$ (shaded hyperboloid) and coherent states of SU(1,1). Dashed black curves mark intelligent coherent states. Ellipses denote the ΔK_x and ΔK_y variances for nine intelligent coherent states. Whereas the atomic vacuum [yellow disk at $(0, 0, 1)$] is a minimum uncertainty state with equal variance in the $\mathcal{K}_x$ and $\mathcal{K}_y$ directions, other intelligent states (magenta ellipses) are squeezed.

$$\langle K_z \rangle = k \cosh \theta, \tag{53}$$

so that the motion of the vector $\langle \mathbf{K} \rangle$ is restricted to the $\langle K_z \rangle > 0$ sheet of the two-sheet hyperboloid $\langle K_z \rangle^2 - \langle K_x \rangle^2 - \langle K_y \rangle^2 = k^2$ (see Fig. 2), as could be expected from the SU(1,1) Casimir in Eq. (29). The variance of the SU(1,1) generators for the coherent states (50) are given by

$$\Delta K_x^2 = \frac{k}{2}(1 + \sinh^2 \theta \cos^2 \phi), \tag{54}$$

$$\Delta K_y^2 = \frac{k}{2}(1 + \sinh^2 \theta \sin^2 \phi), \tag{55}$$

$$\Delta K_z^2 = \frac{k}{2}\sinh^2 \theta. \tag{56}$$

Due to the possibility of multiple occupation in any single mode, neither the expectation values nor the variance of the $\mathbf{K}$ operators are bound. Since the structure constants of the two algebras differ only in sign, the uncertainty relations of SU(1,1) are the same as for SU(2), e.g.,

$$\Delta K_x \Delta K_y \geq \frac{1}{2} |\langle K_z \rangle|, \tag{57}$$

and we can define intelligent and minimum-uncertainty states as we did for SU(2) in the previous subsection. In Fig. 2 we plot the expectation values of $\mathbf{K}$ for SU(2) coherent states, as well as the ΔK_x and ΔK_y variance of nine such states. It is clear from Eqs. (54), (55), and (53) that the intelligent states will be obtained for $\phi = 0$, $\pi/2$, π, and arbitrary θ.

C. Generalized squeezing

The uncertainty equations (46) and (57), demonstrate that the minimum fluctuation product of two of the observables

generating the pertinent Lie algebra, depends on the expectation value of the remaining generator

$$\Delta X_i^2 \leq \frac{1}{2}|c_{ij}^k \langle \hat{X}_k \rangle| \quad \text{and} \quad \Delta X_j^2 \geq \frac{1}{2}|c_{ij}^k \langle \hat{X}_k \rangle|. \quad (58)$$

Generalized squeezed states of Lie algebras generated by $\{\hat{X}_i\}_{i=1,2,3}$ are defined as those states for which the variance in one observable has been reduced at the expense of another [25].

It is clear from Eqs. (39)–(44) that starting from a fermionic atomic vacuum and inducing a rotation about the J_x axis (e.g., by choosing $\Delta=0$ and $g=g^*$), the variance ΔJ_y will be squeezed at the expense of ΔJ_x fluctuations (see Fig. 1) because $1-\sin^2\theta \leq |\cos\theta|$ for all θ. Similarly, rotating about the J_y axis (e.g., by choosing $\Delta=0$ and $g=-g^*$) will result in generalized squeezing of ΔJ_x. The reverse is true for rotations of a boson atomic vacuum, as seen from Eqs. (51)–(56). Starting from the vacuum state (yellow disk in Fig. 2), evolution perpendicular to the K_x axis results in squeezing of ΔK_x, whereas evolution perpendicular to the K_y axis, squeezes ΔK_y. The way to attain this generalized squeezing for fermions and bosons is quite different. Whereas with fermion atoms, squeezing in ΔJ_x is obtained by reduction of these fluctuations, keeping a fixed ΔJ_y variance (thereby reducing the product $\Delta J_x \Delta J_y = |J_z|/2$), the same goal is attained for boson atoms by increasing the variance of K_y (thereby increasing $\Delta K_x \Delta K_y = |K_z|/2$) and keeping K_x fluctuations fixed.

IV. SHORT TIME DYNAMICS

Since the atomic vacuum state (yellow disk in Figs. 1 and 2) is a coherent state, the atomic states produced in the dissociation of a molecular BEC will initially be coherent states of SU(1,1) if the constituent atoms are bosons or of SU(2) when the constituent atoms are fermions. There should thus be a significant difference in the short-time dynamics and in the initial fluctuations between the two cases. For bosons, Eqs. (53) and (56) predict, respectively, the hyperbolic amplification of atom-number and atom number fluctuations, whereas fermion number growth [Eq. (41)] is trigonometric and fluctuations remain bound [Eq. (44)]. Moreover, phase fluctuations initially decrease to zero while atom-number fluctuations approach $\sqrt{j/2}$, indicating the formation of the Glauber coherent state of the Heisenberg-Weyl algebra. Physically, the source of these differences is in the underlying mechanisms of Bose-stimulation of dissociating boson pairs, leading to the dynamical instability of the atomic vacuum, and Pauli blocking of dissociating fermion pairs.

In order to verify the formation of such coherent states and generalized squeezing, we have carried out many-particle simulations of molecular BEC dissociation into either fermionic or bosonic constituent atoms. For sufficiently short propagation times the molecular field is to a good approximation undepleted, and the generalized operators $\mathcal{J}_i, \mathcal{K}_i$ coincide, up to an insignificant c number, with the SU generators J_i, K_i. The atomic states during the initial stage of dissociation are thus approximately SU(2) and SU(1,1) co-
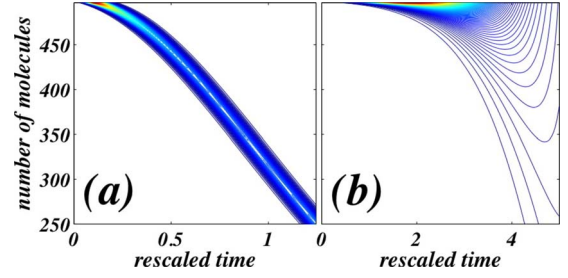

FIG. 3. (Color online) Number distributions as a function of rescaled time in the dissociation of 500 molecules into fermion (a) and boson (b) constituent atoms.

herent states, respectively, for fermion and boson constituents. In what follows, we shall numerically investigate to what extent do the generalized coherent states and squeezed fluctuations depicted in Sec. III for an undepleted pump approximation, carry through to the operators $\mathcal{J}_i, \mathcal{K}_i$, which account for pump depletion and fluctuations. In Fig. 3, we plot the atom-number distribution as a function of the rescaled time $\tau = g\sqrt{N}t$. The dissociation into fermion constituents shown in Fig. 3(a), exhibits the evolution into the Glauber Poissonian number distribution with bound fluctuations, in agreement with Eqs. (41) and (44). Dissociation into boson constituents however, results in a super-Poissonian number distribution with the anticipated hyperbolic growth of fluctuations of Eqs. (53) and (56).

Generalized SU(2) squeezing and its extension into the depleted-pump regime is illustrated in Figs. 4 and 5, where the variance in $\mathcal{J}_x$ and $\mathcal{J}_y$ in the dynamical evolution of the (fermion) atomic vacuum state, are plotted as a function of time. In Fig. 4, the phase of the association pump is $\varphi=0$, corresponding to rotation about the u axis of the Bloch sphere of Fig. 1, i.e., $\phi=\pi/2$. The coalescence of the variance product $\Delta\mathcal{J}_x\Delta\mathcal{J}_y$ with the expectation value of the com-
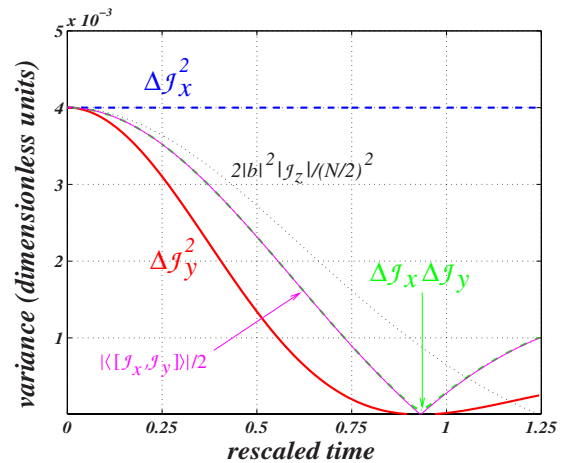

FIG. 4. (Color online) Quadrature variances $\Delta\mathcal{J}_x^2$ (dashed blue line), $\Delta\mathcal{J}_y^2$ (bold solid red line), and $\Delta\mathcal{J}_x\Delta\mathcal{J}_y$ (dash-dotted green line) as a function of the rescaled time $g\sqrt{N}t$, in the dissociation of a molecular BEC made of fermion-dimers. Pump phase is $\varphi=0$. The thin solid magenta line denotes the uncertainty limit $|\langle[\mathcal{J}_x,\mathcal{J}_y]\rangle|/2$ which can be approximated at early times to be $2|b|^2|\mathcal{J}_z|/(N/2)^2$ (dotted black curve).
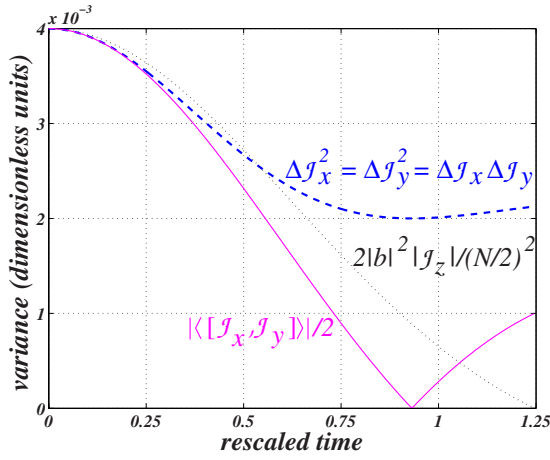
FIG. 5. (Color online) Same as Fig. 3, with pump phase $\varphi = \pi/4$. Quadrature variances $\Delta\mathcal{J}_x^2$, $\Delta\mathcal{J}_y^2$, $\Delta\mathcal{J}_x\Delta\mathcal{J}_y$ (dashed blue line) are all equal and greater than the uncertainty limit $|\langle[\mathcal{J}_x,\mathcal{J}_y]\rangle|/2$ (solid magenta curve) or its short-time approximation $2|b|^2|\mathcal{J}_z|/(N/2)^2$ (dotted black curve).

mutator $\langle[\mathcal{J}_x,\mathcal{J}_y]\rangle$ demonstrates that the generated SU(2) coherent state is indeed intelligent. Squeezing of the $\Delta\mathcal{J}_y$ variance while keeping a fixed $\Delta\mathcal{J}_x$ is observed, in agreement with the undepleted pump prediction. This reduction of $\mathcal{J}_y$ fluctuations eventually results in the expected minimum uncertainty state with $\Delta\mathcal{J}_x\Delta\mathcal{J}_y \approx 0$. In comparison, the evolution of variances for a $\varphi = \pi/4$ phase of the pump (corresponding to rotation along the $\phi = 3\pi/4$ circle on the Bloch sphere of Fig. 1) is shown in Fig. 5. The SU(2) coherent states produced during this evolution, are nonintelligent, with equal $\Delta\mathcal{J}_x$ and $\Delta\mathcal{J}_y$ variances whose product is larger than the uncertainty limit.

The time evolution of variances in the propagation of the atomic vacuum state for boson atoms, with $\varphi = 0, \pi/4$, is shown, respectively, in Figs. 6 and 7. Unlike the fermion case where fluctuations are bound, we observed for $\varphi = 0$ a rapid increase in the $\Delta\mathcal{K}_y$ variance with a fixed $\Delta\mathcal{K}_x$, corre-

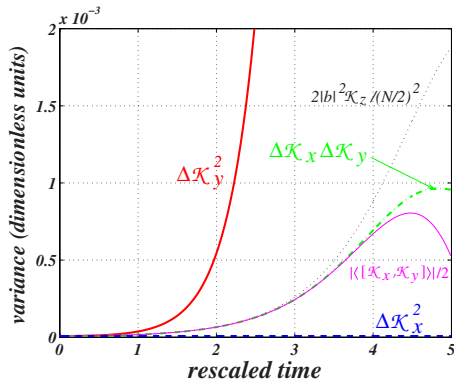FIG. 6. (Color online) Quadrature variances $\Delta\mathcal{K}_x^2$ (dashed blue curve), $\Delta\mathcal{K}_y^2$ (bold solid red curve), and $\Delta\mathcal{K}_x\Delta\mathcal{K}_y$ (dash-dotted green curve) as a function of the rescaled time $g\sqrt{N}t$, in the dissociation of a molecular BEC made of boson dimers. Pump phase is $\varphi = 0$. The solid magenta curve denotes the uncertainty limit $|\langle[\mathcal{K}_x,\mathcal{K}_y]\rangle|/2$ which coincides with $4|b|^2|\mathcal{K}_z|/(N/2)^2$ (dotted black curve) at early times where molecular depletion is negligible.
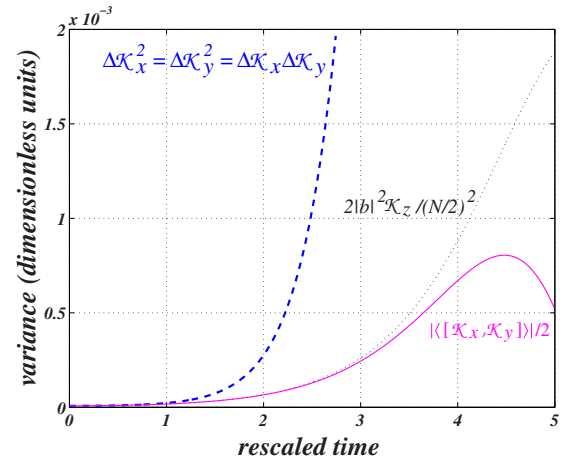

FIG. 7. (Color online) Same as Fig. 4, with pump phase $\varphi = \pi/4$. Quadrature variances $\Delta\mathcal{K}_x^2$, $\Delta\mathcal{K}_y^2$, $\Delta\mathcal{K}_x\Delta\mathcal{K}_y$ (dashed blue) are all equal and greater than the uncertainty limit $|\langle[\mathcal{K}_x,\mathcal{K}_y]\rangle|/2$ (solid magenta) or its short-time approximation $2|b|^2|\mathcal{K}_z|/(N/2)^2$ (dotted black).

sponding to motion on the $\phi = \pi/2$ hyperbola in Fig. 2. While the variance product $\Delta\mathcal{K}_x\Delta\mathcal{K}_y$ grows exponentially with time, its initial evolution traces the uncertainty limit $|\langle[\mathcal{K}_x,\mathcal{K}_y]\rangle|/2$ indicating that the produced states are indeed SU(1,1) intelligent coherent states. Here too, propagation with a zero phase of the pump leads to the expected generalized squeezing. For $\varphi = \pi/4$, however, there is no squeezing as both $\Delta\mathcal{K}_x$ and $\Delta\mathcal{K}_y$ fluctuations are equal and hyperbolically growing. The SU(1,1) coherent states produced are nonintelligent because the variance product $\Delta\mathcal{K}_x\Delta\mathcal{K}_y$ is larger than the uncertainty limit.

The agreement between the numerically exact variance dynamics of Figs. 4–7 and the undepleted pump pictures of Figs. 1 and 2, demonstrates that the different collective dynamics predicted for fermion and boson constituent atoms can indeed be interpreted in terms of fluctuations of dynamical variables quadratic in the atomic creation or annihilation operators. The reduction of fluctuations of these variables is related to the formation of coherent states of the SU(2) and SU(1,1) Lie algebras. The same qualitative picture seems to apply to the depleted pump regime.

Finally, the mapping between fermion and boson dynamics, manifested in the equivalence of Eqs. (18)–(20) with $\eta = 1$ and Eq. (35) with $k = 1/2$, is illustrated in Fig. 8 where atom number distributions are plotted as a function of time throughout the association of a Fermi [Fig. 8(a)] and Bose [Fig. 8(b)] atomic quantum gas. Fermion association is mapped onto boson dissociation [Fig. 3(b)] while boson association coincides with fermion dissociation [Fig. 3(a)], generating similar coherent states.

V. SUMMARY AND CONCLUSIONS

We have established a connection between the collective behavior in boson and fermion pairing via Feshbach resonances and the generation of coherent states of the SU(1,1) and SU(2) Lie algebras. This relation provides a new view-
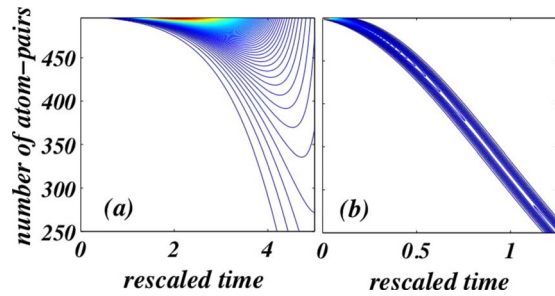
FIG. 8. (Color online) Number distributions as a function of rescaled time for the association of quantum degenerate gases of fermions (a) and bosons (b) with $N=1000$.

point on the quantum statistics of atom-molecule quantum gas processes. The equivalence of molecular BEC dissociation with the Dicke model for fermion atoms [31] and with parametric down-conversion for boson atoms [44], known for some time in the quantum optics literature, is put into context as these two quantum systems are paradigmatic examples of the aforementioned algebras. The well known squeezing of fluctuations in dynamical variables linear in the atomic creation or annihilation operators (e.g., quadrature

squeezing) during the dissociation into boson constituents, may be viewed as generalized $SU(1,1)$ squeezing of pair fluctuations, quadratic in the atomic creation and annihilation operators. Similarly, the coherent evolution during dissociation into fermion atoms corresponds to the generation of a minimum uncertainty $SU(2)$ coherent state. Our numerical simulations indicate that the same qualitative picture applies to the fluctuation of operators that account for molecular pump depletion. The presentation of the atom-molecule system in terms of these generators offers a link between the fermion- and boson-constituent atom cases due to the close relation and direct mapping between the underlying Lie algebras.

[1] H. Feshbach, Ann. Phys. **19**, 287 (1962); H. Feshbach, *Theoretical Nuclear Physics* (Wiley, New York, 1992).

[2] S. Inouye, M. R. Andrews, J. Stenger, H.-J. Miesner, D. M. Staper-Kurn, and W. Ketterle, Nature (London) **392**, 151 (1998).

[3] C. A. Regal, C. Ticknor, J. L. Bohn, and D. S. Jin, Nature (London) **424**, 47 (2003).

[4] M. Greiner, C. A. Regal, and D. S. Jin, Nature (London) **426**, 537 (2003).

[5] S. Jochim, M. Bartenstein, A. Altmeyer, G. Hendl, S. Riedl, C. Chin, J. Hecker Denschlag, and R. Grimm, Science **302**, 2101 (2003).

[6] M. W. Zwierlein, C. A. Stan, C. H. Schunck, S. M. F. Raupach, S. Gupta, Z. Hadzibabic, and W. Ketterle, Phys. Rev. Lett. **91**, 250401 (2003).

[7] N. R. Claussen, E. A. Donley, S. T. Thompson, and C. E. Wieman, Phys. Rev. Lett. **89**, 010401 (2002).

[8] J. Herbig, T. Krämer, M. Mark, T. Weber, C. Chin, H.-C. Nägerl, and R. Grimm, Science **301**, 1510 (2003).

[9] S. Dürr, T. Volz, A. Marte, and G. Rempe, Phys. Rev. Lett. **92**, 020406 (2004).

[10] C. A. Regal, M. Greiner, and D. S. Jin, Phys. Rev. Lett. **92**, 040403 (2004).

[11] M. W. Zwierlein, C. A. Stan, C. H. Schunck, S. M. F. Raupach, A. J. Kerman, and W. Ketterle, Phys. Rev. Lett. **92**, 120403 (2004).

[12] M. Bartenstein, A. Altmeyer, S. Riedl, S. Jochim, C. Chin, J. H. Denschlag, and R. Grimm, Phys. Rev. Lett. **92**, 120401 (2004).

[13] T. Bourdel, L. Khaykovich, J. Cubizolles, J. Zhang, F. Chevy, M. Teichmann, L. Tarruell, S. J. J. M. F. Kokkelmans, and C. Salomon, Phys. Rev. Lett. **93**, 050401 (2004).

[14] J. Kinast, S. L. Hemmer, M. E. Gehm, A. Turlapov, and J. E. Thomas, Phys. Rev. Lett. **92**, 150402 (2004).

[15] C. Chin, M. Bartenstein, A. Altmeyer, S. Riedl, S. Jochim, J. H. Denschlag, and R. Grimm, Science **305**, 1128 (2004).

[16] M. Greiner, C. A. Regal, and D. S. Jin, Phys. Rev. Lett. **94**, 070403 (2005).

[17] M. W. Zwierlein, C. H. Schunck, C. A. Stan, S. M. F. Raupach, and W. Ketterle, Phys. Rev. Lett. **94**, 180401 (2005).

[18] K. V. Kheruntsyan and P. D. Drummond, Phys. Rev. A **66**, 031602(R) (2002).

[19] K. V. Kheruntsyan, Phys. Rev. Lett. **96**, 110401 (2006).

[20] T. Miyakawa and P. Meystre, Phys. Rev. A **71**, 033624 (2005).

[21] D. Meiser, P. Meystre, and C. P. Search, Phys. Rev. A **71**, 033621 (2005).

[22] D. Meiser and P. Meystre, Phys. Rev. Lett. **94**, 093001 (2005).

[23] H. Uys, T. Miyakawa, D. Meiser, and P. Meystre, Phys. Rev. A **72**, 053616 (2005).

[24] M. W. Jack and H. Pu, Phys. Rev. A **72**, 063625 (2005).

[25] K. Wodkiewicz and J. H. Eberly, J. Opt. Soc. Am. B **2**, 458 (1985).

[26] A. V. Andreev, V. Gurarie, and L. Radzihovsky, Phys. Rev. Lett. **93**, 130402 (2004).

[27] R. A. Barankov and L. S. Levitov, Phys. Rev. Lett. **93**, 130403 (2004).

[28] E. Pazy, A. Vardi, and Y. B. Band, Phys. Rev. Lett. **93**, 120409 (2004).

[29] E. Pazy, I. Tikhonenkov, Y. B. Band, M. Fleischhauer, and A. Vardi, Phys. Rev. Lett. **95**, 170403 (2005).

[30] I. Tikhonenkov, E. Pazy, Y. B. Band, M. Fleischhauer, and A. Vardi, Phys. Rev. A **73**, 043605 (2006).

[31] R. H. Dicke, Phys. Rev. **93**, 99 (1954).

[32] P. D. Drummond, K. V. Kheruntsyan, and H. He, Phys. Rev.

Lett. **81**, 3055 (1998).

[33] J. Javanainen and M. Kostrun, Opt. Express **5**, 188 (1999); J. Javanainen and M. Mackie, Phys. Rev. A **59**, R3186 (1999).

[34] D. J. Heinzen, R. Wynar, P. D. Drummond, and K. V. Kheruntsyan, Phys. Rev. Lett. **84**, 5029 (2000).

[35] A. Vardi, V. A. Yurovsky, and J. R. Anglin, Phys. Rev. A **64**, 063611 (2001).

[36] A. Vardi and M. G. Moore, Phys. Rev. Lett. **89**, 090403 (2002).

[37] M. G. Moore and A. Vardi, Phys. Rev. Lett. **88**, 160402 (2002).

[38] I. Tikhonenkov and A. Vardi, Phys. Rev. Lett. **98**, 080403 (2007).

[39] J. J. Hope and M. K. Olsen, Phys. Rev. Lett. **86**, 3220 (2001).

[40] U. V. Poulsen and K. Molmer, Phys. Rev. A **63**, 023604 (2001).

[41] K. V. Kheruntsyan, Phys. Rev. A **71**, 053609 (2005).

[42] C. M. Savage, P. E. Schwenn, and K. V. Kheruntsyan, Phys. Rev. A **74**, 033620 (2006).

[43] C. M. Savage and K. V. Kheruntsyan, Phys. Rev. Lett. **99**, 220404 (2007).

[44] D. F. Walls and G. J. Milburn, *Quantum Optics* (Springer-Verlag, Berlin, 1995), Chap. 5; C. A. Holmes, G. J. Milburn, and D. F. Walls, Phys. Rev. A **39**, 2493 (1989).

[45] I. Tikhonenkov, E. Pazy, and A. Vardi, Opt. Commun. **264**, 321 (2006).

[46] F. T. Arecchi, E. Courtens, R. Gilmore, and H. Thomas, Phys. Rev. A **6**, 2211 (1972); A. M. Perelomov, Commun. Math. Phys. **26**, 222 (1972); Usp. Fiz. Nauk **123**, 23 (1977) [Sov. Phys. Usp. **20**, 703 (1977)].

[47] A. O. Barut and R. Raczka, *Theory of Group Representation and Applications* (Polish Scientific Publishers, Warsaw, 1977).